

Energy- and Charge-Transfer Processes in a Perylene–BODIPY–Pyridine Tripartite Array

Mohammed A. H. Alamiry,^[a] Anthony Harriman,^{*[a]} Laura J. Mallon,^[a] Gilles Ulrich,^[b] and Raymond Ziessel^{*[b]}

Keywords: Energy transfer / Perylene / Fluorescence / Chemical sensor / Boron dipyrromethene dye

A novel boron dipyrromethene (BODIPY) dye has been synthesized in which the F atoms, usually bound to the boron center, have been replaced with 1-ethynylperylene units and a 4-pyridine residue is attached at the *meso*-position. The perylene units function as photon collectors over the wavelength range from 350 to 480 nm. Despite an unfavorable spectral overlap integral, rapid energy transfer takes place from the singlet-excited state of the perylene unit to the adjacent BODIPY residue, which is itself strongly fluorescent. The mean energy-transfer time is 7 ± 2 ps at room temperature. The dominant mechanism for the energy-transfer process is Dexter-type electron exchange, with Förster-type dipole–dipole interactions accounting for less than 10 % of the total transfer probability. There are no indications for light-induced electron transfer in this system, although there is evidence for a nonradiative decay channel not normally seen

for *F*-type BODIPY dyes. This new escape route is further exposed by the application of high pressure. The *meso*-pyridine group is a passive bystander until protons are added to the system. Then, protonation of the pyridine N atom leads to complete extinction of fluorescence from the BODIPY dye and slight recovery of fluorescence from the perylene units. Quenching of BODIPY-based fluorescence is due to charge-transfer to the pyridinium unit whereas the re-appearance of perylene-based emission is caused by a reduction in the Förster overlap integral upon protonation. Other cations, most notably zinc(II) ions, bind to the pyridine N-atom and induce similar effects but the resultant conjugate is weakly fluorescent.

(© Wiley-VCH Verlag GmbH & Co. KGaA, 69451 Weinheim, Germany, 2008)

Introduction

The last few decades have witnessed the rationale development of many different luminescent sensors for the sensitive, and sometimes selective, recognition of certain chemical species in solution. A tremendous wealth of information has accrued and some invaluable lessons have been learned with respect to the basic design principles.^[1–3] Most notable among the major strategies used to introduce an on/off switching device has been light-induced electron transfer, usually involving an amine donor covalently attached close to a fluorescent molecule.^[4] Two complementary approaches can be considered within this overall scheme. Thus, binding of the analyte can curtail electron transfer, thereby leading to restoration of the emission inherent to the chromophore,^[5] or the opposite behavior can be engineered so that binding switches off the emission.^[4] Each route has benefits and disadvantages, according to the nature of

the targeted substrate, but it is clear that the recognition event must be accompanied by definitive on-off signaling. We now report on a general purpose fluorescent sensor designed specifically to monitor high concentrations of cations in an effluent stream. Such systems are intended as companion monitors for probes that detect low and/or medium range levels of pollutants and should be considered as the final overload device for an integrated network of sensors. That is to say, a sensitive probe sends out a warning signal that a pollutant is present. A network of secondary sensors monitors the rising concentration of pollutant until the point when the final sensor is triggered. At this point, a termination signal is sent to the operations panel.

As a major breakthrough over the past few years, boron dipyrromethene dyes have emerged as a versatile, robust and easily modified class of fluorescent reagent.^[6] These materials display little inclination to undergo intersystem crossing to the triplet manifold and exhibit fluorescence properties that are relatively insensitive to changes in the local environment. Fluorescence quantum yields are usually high but the excited-state lifetimes are too short to be affected by the presence of dissolved oxygen. A problem found for earlier derivatives in that the Stokes' shift is too small for practical exploitation of the dye as a fluorescent probe can be overcome by covalent attachment^[7] of secondary

[a] Molecular Photonics Laboratory, School of Natural Sciences, Bedson Building, Newcastle University, Newcastle upon Tyne, NE1 7RU, UK
E-mail: anthony.harriman@ncl.ac.uk

[b] Laboratoire de Chimie Moléculaire, Centre National de la Recherche Scientifique (CNRS), École de Chimie, Polymères, Matériaux (ECPM),
25 rue Becquerel, 67087 Strasbourg Cedex 02, France

chromophores that expand the range of excitation wavelengths. In this regard, it is important to note the benefits associated with functionalization at the boron center.^[8] In the sensor described below, we use this latter strategy to attach ethynylated perylene units to the boron dipyrromethene (BODIPY) dye for precisely this reason.

Regarding the recognition unit, we return to a molecular dyad reported recently in which the BODIPY dye is equipped with a *meso* *N*-methylpyridinium unit.^[9] This electron-affinic residue quenches fluorescence from the BODIPY dye due to the onset of a light-induced charge-transfer process that is unavailable to the simpler pyridine derivative. Our presumption here is that the *N*-methyl group might be replaced with cationic species, including protons, which will also serve as quenchers for the BODIPY emission. Since pyridine is not a particularly effective coordination reagent, we might expect the stability constants for complexation of cations from solution to be relatively low. If so, this fulfills the basic design element essential for a fluorescent terminator of the type highlighted above. We now describe the synthesis, photophysical properties and preliminary binding characteristics of a prototypic dye of this general class.

Results and Discussion

Synthesis

The synthesis of compound **1** has been described previously and involves condensation of kryptopyrrole with 4-formylpyridine.^[10] An acceptable yield is obtained on a routine basis using 4-(chlorocarbonyl)pyridine as the starting point for a one-pot synthesis. Two pyrrole molecules are condensed over four days with the acetyl chloride, to form the corresponding dipyrromethene hydrochloride salts. Deprotonation with a tertiary amine, followed by addition of boron difluoride, allows formation of the boron complex **1** in 40% yield. Substitution of the two fluorine atoms of the boradiazaindacene dye **1** is achieved by addition of the corresponding acetylenic Grignard reagent and subsequent heating at 60 °C. Work-up and standard purification pro-

cedures afforded the analytically pure dyes **2** and **3** in modest yields. The compounds **1** and **2** are used as reference materials by which to better understand the properties of the perylene-based dye **3** (Scheme 1).

Photophysics of **3**

The absorption spectrum of **3** in CH₂Cl₂ (Figure 1) shows a transition located at ca. 465 nm that can be assigned to the perylene S₀→S₁ transition.^[11] Also present in the absorption spectrum is the S₀→S₁ transition of the BODIPY chromophore that is centered at ca. 525 nm.^[12] The S₀→S₂ transition associated with the BODIPY unit lies underneath the more intense perylene S₀→S₁ bands.^[13] The absorption bands are sharp, well-resolved and located at similar positions to those found for appropriate reference compounds, which suggests that the perylene and BODIPY units are not in strong electronic communication. This finding is in agreement with earlier work carried out with B-linked molecular dyads.^[6] Close comparison of the absorption spectrum of **3** with those of the respective reference compounds indicates that the perylene S₀→S₁ band undergoes a red shift of ca. 2 nm while the S₀→S₁ band for the BODIPY unit is red-shifted by ca. 6 nm. On integration of the molar absorption coefficients measured for **1** and **3** it can be concluded that the presence of the perylene units leads to a 2.6-fold increase in the number of photons that can be collected.

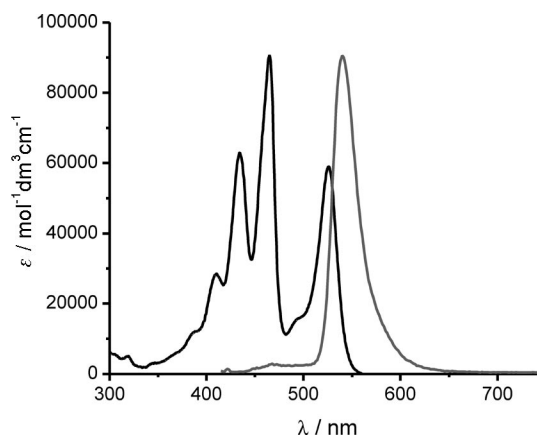
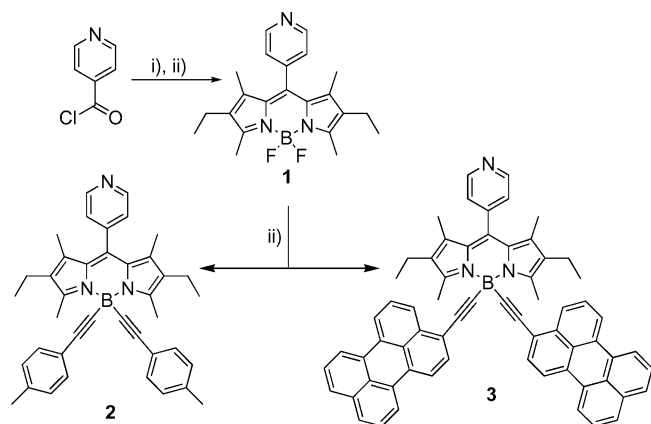


Figure 1. Absorption (black) and emission (grey) spectra recorded for **3** in CH₂Cl₂ solution at room temperature. The excitation wavelength used for the fluorescence spectrum was 408 nm.



Scheme 1. i) Kryptopyrrole (2 equiv.), CH₂Cl₂, room temp.; ii) TEA, BF₃·OEt₂; iii) R≡MgBr (2.5 equiv.), THF, 60 °C.

The fluorescence spectrum recorded for **3** in CH₂Cl₂ (Figure 1) shows emission from the BODIPY unit, centered at 540 nm,^[12] but some residual fluorescence from the perylene unit^[11] can be seen within the window between 450 and 500 nm. The fluorescence quantum yield (Φ_F) measured for the BODIPY unit in CH₂Cl₂ was found to be 0.31, which is somewhat reduced relative to **1** (Φ_F = 0.58). Likewise, the excited-singlet-state lifetime (τ_S = 2.6 ns) for the BODIPY unit remains about half of those recorded for the reference compounds **1** (τ_S = 5.4 ns) and **2** (τ_S = 4.9 ns). Even so, the decay traces fit well to mono-exponential ki-

netics. The radiative rate constant (k_{RAD}) found for **3** is $1.3 \times 10^8 \text{ s}^{-1}$ and is in excellent agreement with that calculated from the Strickler–Berg expression^[14] ($k_{\text{RAD}} = 1.2 \times 10^8 \text{ s}^{-1}$). Fluorescence from the BODIPY unit shows good mirror symmetry with the corresponding absorption spectral profile and the Stokes' shift is modest. The corrected fluorescence excitation spectrum agrees well with the absorption spectrum recorded over the region from 250 to 520 nm and it is clear that photons absorbed by the perylene units are transferred to the BODIPY unit with high efficiency. Nonetheless there is a clear sense that **3** is subject to an additional nonradiative channel that remains closed to the conventional *F*-BODIPY dyes and that somehow involves the perylene units.^[6] The exact nature of this new decay route is unknown but might involve large scale torsional motion of the appendages because the effect appears to increase proportionally with the bulk of the B-based substituents. More work is required to better clarify this effect, which is currently being examined by high-pressure studies on derivatives not able to undergo intramolecular energy transfer.

The small residual fluorescence from the perylene units (Figure 1) corresponds to an amount of around 0.1% of that found for 1-ethynylperylene in CH_2Cl_2 at room temperature ($\Phi_{\text{F}} = 0.79$) with excitation at 435 nm. Time-correlated, single-photon counting studies with a temporal resolution of ca. 50 ps and using a variety of emission and excitation wavelengths failed to detect any emission from the perylene unit in CH_2Cl_2 , indicating that $\tau_{\text{S}} < 40 \text{ ps}$. Similar results were found in other solvents, including methyltetrahydrofuran, cyclohexane and acetonitrile, and at all suitable excitation wavelengths. From this, it can be deduced that efficient energy transfer occurs from the perylene units to the nearby BODIPY residue.^[15–17] On the basis of the time-resolved emission studies, the rate constant for intramolecular energy transfer (k_{EiT}) must exceed ca. $2.5 \times 10^{10} \text{ s}^{-1}$.

Using improved temporal resolution, k_{EiT} was found to be $1.4 \times 10^{11} \text{ s}^{-1}$ in CH_2Cl_2 solution at room temperature. This latter study involved excitation of the perylene unit at 420 nm with a sub-ps laser pulse (FWHM = 0.22 ps) and monitoring bleaching of the S_0 – S_1 absorption transition associated with the BODIPY unit (Figure 2). It is clear that the bulk of the bleaching signal occurs on time scales much longer than that of the excitation pulse. The bleaching kinetics are not well described by a single exponential step, however, and the quoted rate constant is the mean value that corresponds to the reciprocal of the time taken for the signal to reach 1/e of its initial value. The mean lifetime found for the singlet-excited state of the perylene unit was $7 \pm 2 \text{ ps}$. The BODIPY S_1 state shows a small amount (i.e., 10%) of decay over 40 ps but the residual signal is not deactivated on time scales less than several hundred picoseconds.

The two mechanisms normally invoked to account for electronic energy transfer are the Förster (dipole–dipole, through space) and Dexter (electron exchange, through bond) processes. Both these mechanisms have been observed with BODIPY dyes equipped with aryl hydrocarbon

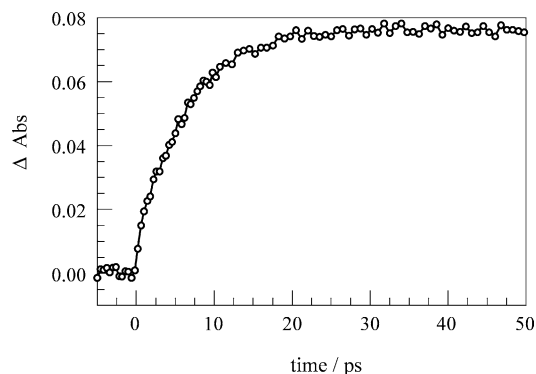


Figure 2. A kinetic trace showing depletion of the ground state of the BODIPY unit following laser excitation into one of the perylene residues at 420 nm. The trace was recorded at 515 nm.

appendages. Thus, Burgess et al.^[16] have reported rapid electron exchange for certain *meso*-substituted BODIPY dyes while Harriman et al.^[17] have described dipole–dipole energy transfer for some B-substituted BODIPY dyes. For **3**, there is strong spectral overlap between fluorescence from the perylene unit and absorption by the BODIPY residue. The Förster overlap integral (J_{F}) calculated from the reference compounds is $1.16 \times 10^{-13} \text{ mol}^{-1} \text{ cm}^6$. The average center-to-center separation distance derived from molecular dynamics simulations^[17] (MDS) is 15.6 Å, while the quantum yield ($\Phi_{\text{F}} = 0.79$) and excited-singlet lifetime ($\tau_{\text{S}} = 4.5 \text{ ns}$) of the donor are known from separate studies. Fluctuations around the connecting B–C bond and slight structural distortions associated with the perylene residue cause a modest range of Förster-type orientation factors (κ). The mean κ value obtained from MDS runs is 0.21, which is rather small and much below the value ($\kappa^2 = 0.67$) appropriate for random orientations. Using these various values in conjunction with the Förster expression leads to an estimated rate constant for dipole–dipole energy transfer (k_{F}) of $1.3 \times 10^{10} \text{ s}^{-1}$. Although very high, this rate constant is too low to satisfactorily account for the measured value. We conclude, therefore, that intramolecular energy transfer in **3** involves both electron exchange ($k_{\text{D}} = 12.7 \times 10^{10} \text{ s}^{-1}$) and dipole–dipole ($k_{\text{F}} = 1.3 \times 10^{10} \text{ s}^{-1}$) mechanisms. For the specific molecule under consideration, it appears that Dexter-type electron exchange is by far the dominant mechanism. This situation is reminiscent of the *meso*-anthracene substituted BODIPY dyes described by Burgess et al.^[16]

Effect of High Pressure

Further insight into the nature of the additional nonradiative decay channel available to **3** but closed to conventional *F*-BODIPY dyes was sought from fluorescence studies performed at high applied pressure. This approach was taken because of suspicions that the large appendages might impose changes in the geometry of the BODIPY unit, especially at the excited-state level.^[18] It was found that the fluorescence intensity for the corresponding *F*-BODIPY derivative fitted with a *meso*-phenyl group increased slightly when

a solution in methyltetrahydrofuran (MTHF) was exposed to high pressure. This effect was quite modest, however, and corresponds to an increase of ca. 5% for an applied pressure of 550 MPa. It is caused by a small reduction in the volume of the solvent.^[19] There was also a red shift in the emission peak, amounting to ca. 5 nm at 550 MPa, due to the pressure-induced change in solvent polarisability.^[20] Surprisingly, applying pressure to a dilute solution of **3** in MTHF causes a serious decrease in fluorescence from the BODIPY unit but a small increase in fluorescence from the perylene units (Figure 3). This experiment refers to excitation into the perylene subunits at 408 nm. It is noticeable that an isoemissive point at 522 nm is preserved during the pressure changes and that the system is both reversible and reproducible.

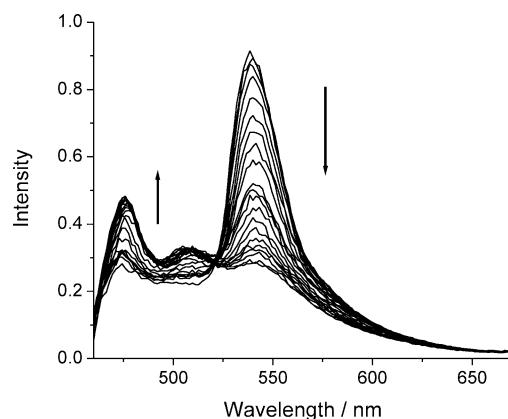


Figure 3. The effect of applied pressure (in even steps up to 550 MPa) on the fluorescence spectrum of **3** in MTHF, following excitation at 408 nm. With increasing pressure, the signal attributed to perylene increases while that due to BODIPY decreases.

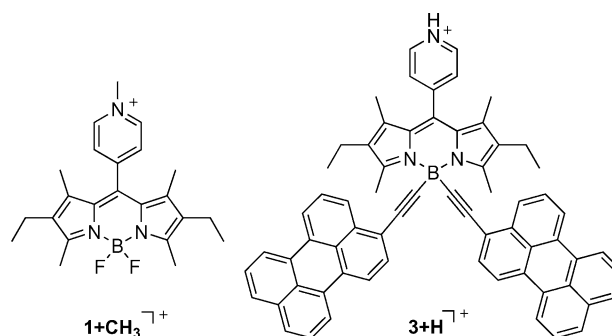
The enhanced fluorescence from the perylene units seen at high pressure must be a consequence of a decreased rate of intramolecular energy transfer. In turn, this situation arises because of a pressure-induced change in the molecular geometry, the precise nature of which cannot be explained on the basis of these experiments alone. This is because a change in geometry could easily affect the probabilities of both Förster and Dexter mechanisms while a similar effect would result from freezing the structure into the lowest-energy conformation. The increase in perylene-based emission is a factor of ca. 10-fold at 550 MPa in MTHF. Restricted energy transfer would account for a modest drop in fluorescence from the BODIPY unit but the actual decrease observed is far too high to be explained solely in this way. The residual BODIPY-based emission is red-shifted by ca. 8 nm, again indicating the change in polarisability of the solvent,^[20] but not significantly broadened. Related experiments show that the absorption spectrum undergoes a red shift of 6 nm but no observable decrease. Loss of fluorescence, therefore, is not due to marked effects imposed at the ground-state level.

A full description of this pressure-sensitive nonradiative decay channel must await a more detailed investigation but

a few comments are in order here. A possible explanation has the perylene appendages acting as levers by which to perturb the geometry around the upper rim of the dipyrroin unit. A similar effect has been described^[21] for *F*-BODIPY dyes lacking the bulky alkyl groups on the pyrrole nucleus. Such structural distortion allows the *meso*-phenyl ring to rotate in the excited state and, by way of holes in the potential surface, facilitates fast nonradiative decay to the ground state.^[22] We invoke a similar effect here as the reason why **3** is somewhat less fluorescent than expected. It then remains for the amount of structural distortion to increase systematically with increasing pressure. This is a mechanical effect.

Protonation of **3**

Earlier work^[9] has shown that alkylation of the pyridine N atom present in **1** switches-on a light-induced charge-transfer reaction in which the *N*-alkyl pyridinium unit acts as acceptor and the singlet-excited state of the BODIPY unit functions as donor. The charge-transfer state (CTS) is weakly fluorescent. Addition of protons to a solution of **3** (Scheme 2) results in extinction of fluorescence from the BODIPY unit (Figure 4). This effect is independent of the nature of the proton source and insensitive to the choice of solvent. The protonated analogue does not fluoresce, at least with any appreciable yield or lifetime. Protonation, which is assumed to take place at the pyridine N atom, is fully reversible and does not cause chemical damage to the molecule. Inappropriate counteranions, however, facilitate precipitation of the protonated species. The data collected from sets of fluorescence spectral titrations allow calculation of the stability constant (β) for the monoprotonated species as being $400 \pm 20 \text{ M}^{-1}$ in methyltetrahydrofuran solution. Higher-order protonation was not observed during these titrations. Accurate fitting of the data could be achieved with the fluorescence quantum yield for the protonated species being set equal to zero; that is to say, only the pyridine form fluoresces to any significant degree. Concomitant with fluorescence quenching, the absorption spectrum recorded for the BODIPY unit undergoes a red shift of ca. 12 nm but that of the perylene unit remains unaffected.



Scheme 2.

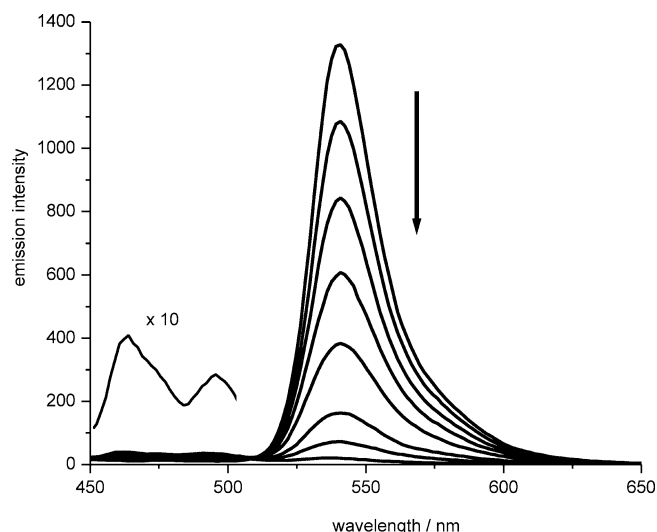


Figure 4. The fluorescence spectrum of **3** in methyltetrahydrofuran solution recorded as a function of incremental additions of triflic acid. The insert shows a 10-fold expanded version of the perylene fluorescence region, as observed in the presence of excess acid.

An interesting feature of the protonation of **3** in methyltetrahydrofuran solution relates to the partial recovery of fluorescence associated with the perylene unit (Figure 4), similar to that seen at high pressure. Thus, when the pyridine unit is protonated the fluorescence quantum yield for emission from the perylene unit is raised from 0.1% to 0.5%. This fivefold increase in Φ_F is highly reproducible and essentially independent of the nature of the solvent. The fluorescence enhancement can be traced to a decreased Förster overlap integral caused by the red-shifted absorption spectral profile for the BODIPY-based acceptor. Indeed, protonation of the pyridine N atom reduces J_F by ca. 15% and thereby minimizes the contribution of dipole–dipole energy transfer. The calculated rate constant for Förster-type energy transfer ($k_F = 1.1 \times 10^{10} \text{ s}^{-1}$) following protonation agrees very well with the decrease in the overall rate constant on the assumption that the Dexter process remains unaffected. Although the effect is small, the ability to switch on fluorescence from the ancillary light harvester during the sensing process holds promise for the future design on improved orthogonal probes. It might be noted that precisely the same effect is found with weaker acids, including trifluoroacetic acid.

The mechanism whereby **3** registers the presence of protons in solution can be explained in terms of an internal charge-transfer process that is available only to the protonated species. This behavior is similar to that noted previously for the N-alkylated derivative of **1**,^[9] except that the protonated species is non-fluorescent. Alkylation or protonation of the pyridine N atom raises the reduction potential for one-electron reduction of this moiety to a much less negative value and thereby switches on the light-induced charge-transfer step. Following methylation of the pyridine N atom, there is a thermodynamic driving force of ca. 0.12 eV for reduction of the pyridinium unit by the first-

excited singlet state of the BODIPY unit and charge transfer occurs on a time scale of ca. 5 ps.^[9] Cyclic voltammetry studies performed with the protonated analogue showed the reduction step to be irreversible but did confirm that intramolecular charge transfer is likely to compete with radiative decay of the BODIPY-based singlet-excited state, at least on thermodynamic grounds. Laser excitation into the perylene unit at 420 nm leads to rapid bleaching of the S_0 – S_1 absorption transition localized on the BODIPY dye. Again, the mean lifetime for the energy-transfer step was of the order of 7 ± 2 ps. In this case, however, the S_1 state localized on the BODIPY unit reverts to the ground state with a lifetime of 42 ± 4 ps (Figure 5). This is substantially shorter than that found for either the parent compound **3** ($\tau_S = 2.6$ ns) or the charge-transfer state observed for the N-methylpyridinium analogue ($\tau_{CTS} = 0.52$ ns in acetonitrile).^[9] On the basis that quenching of the BODIPY S_1 state occurs exclusively by way of intramolecular charge transfer, we can establish the rate constant for this step as being $2.4 \times 10^{10} \text{ s}^{-1}$. Since the resultant charge-transfer state cannot be resolved in the decay records, it follows that charge recombination must occur on a faster time scale. The remarkable difference in lifetimes for the charge-transfer states found for methylated ($\tau_{CTS} = 0.52$ ns) and protonated ($\tau_{CTS} < 40$ ps species), allowing for the different nature of the BODIPY unit (i.e., **1** vs. **3**), indicates that the N–H group must promote rapid nonradiative deactivation of the charge-transfer state. This observation is in line with the energy-gap law.^[23]

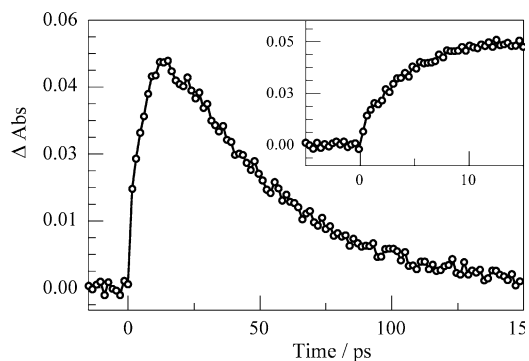


Figure 5. Kinetic trace recorded at 520 nm following laser excitation of the protonated form of **3** and showing the depletion of the ground state of the BODIPY unit. The insert shows an expanded version of the early time period.

Several other BODIPY-based dyes are known to function as pH indicators whereby protonation switches off a charge-transfer reaction and restores fluorescence.^[24] Compound **3** complements these probes by functioning primarily in acid solution and using protonation to switch off the radiative process. Many of the other proton sensors employ an electron-donating amine as the protonation site and benefit from high binding constants (e.g., $\beta > 10^5 \text{ M}^{-1}$). Such dyes are useful for measuring low concentrations of acid whereas **3** will operate best in proton-rich environments. This is precisely in accord with our main design requisite.

Coordination of Metal Cations

Many different cations will coordinate to the pyridine N atom so as to form a stable complex, for which the binding constants vary over a very wide range. There is little, if any, selectivity for the binding event. It was noted that **3** forms a ground-state complex with a selection of metal cations. In each case, complexation affected the absorption and fluorescence spectra. We now describe the results observed on addition of zinc(II) ions to a solution of **3** in methyltetrahydrofuran as being representative of these cations. Thus, in the presence of a small excess of zinc perchlorate, the absorption spectrum recorded for **3** shows a pronounced red shift and broadening for the bands associated with the BODIPY unit. This shift is on the order of 10 nm but little change is observed for the transitions localized on the perylene unit (Figure 6). The fluorescence yield, measured after excitation into the BODIPY unit, is decreased in the presence of zinc(II) ions and reaches a limiting value on addition of a large excess of the salt that corresponds to ca. 30% of that of the non-coordinated compound. Interestingly, and unlike the situation that follows from protonation of **3**, the residual fluorescence spectrum is red-shifted by ca. 10 nm (Figure 7). This latter spectrum is characteristic of the zinc(II) – **3** conjugate. The fluorescence lifetime recorded for this complex is 1.2 ns. Again, there is a definite increase in fluorescence from the perylene unit due to the reduced Förster spectral overlap integral associated with the red-shifted absorption spectrum of the BODIPY-based acceptor. In this case, the spectral shift is sufficient to virtually extinguish the Förster contribution.

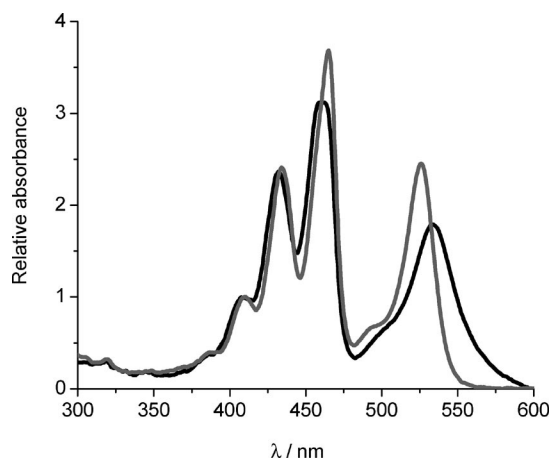


Figure 6. Effect of the presence of zinc(II) cations on the absorption spectrum recorded for **3** in methyltetrahydrofuran; before addition (grey curve) and after addition (black curve) of zinc perchlorate.

In marked contrast to the protonated species, the conjugate formed between **3** and zinc(II) cations fluoresces in fluid solution at room temperature.^[25] The emission spectrum is red-shifted and broadened, in agreement with the modified absorption spectrum, while the excitation spectrum shows good correspondence with the absorption spectrum recorded over the visible and near-UV regions. The

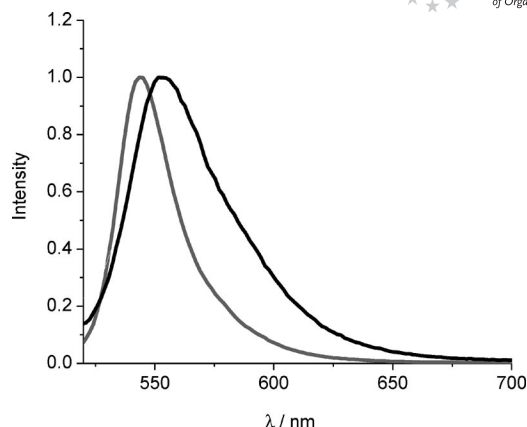


Figure 7. Effect of added zinc(II) cations on the fluorescence spectrum recorded for **3** in methyltetrahydrofuran; before addition (grey curve) and after addition (black curve) of zinc perchlorate.

emission spectrum does not change on addition of excess zinc(II) cations and is independent of the nature of the counterion. Cyclic voltammetry shows that light-induced charge-transfer is unlikely to take place for the zinc(II) complex, at least on thermodynamic grounds. Consequently, the observed effect of coordination of the metal ion to the pyridine N atom can be attributed to an electronic factor. The somewhat enhanced rate of decay of the fluorescent conjugate is possibly because of spin-orbit coupling associated with the zinc(II) ion.

Conclusions

The ancillary perylene units appended to the previously reported BODIPY-based dye **1** allows harvesting of photons in the 350–480 nm window, where the dye is relatively transparent. These photon collectors, being attached by ethyne linkers to the B center, display fast energy transfer to the BODIPY core via both through-bond and through-space mechanisms. As reported before, the presence of large polycyclic hydrocarbons in place of the usual F atoms leads to a modest increase in the rate of nonradiative decay of the excited singlet state of the BODIPY unit.^[22] This process is highly sensitive to applied pressure, although the actual details for this effect are unclear at present. The polycycle is free to rotate around the connecting ethyne group, but there is poor alignment of the transition dipoles and this minimizes Förster-type energy transfer to the BODIPY unit. This effect is offset, however, by the effective electronic coupling supplied by the linkage that facilitates fast through-bond energy transfer. This realization opens the way to design improved photon collectors built from multiple units that combine to cover much of the spectral range.^[26] It should also be noted that the conjugation length of the BODIPY dye is extended when suitable groups are attached to the pyrrole rings.^[27,28] In this way, most of the visible region can be harvested. This simple strategy serves to enlarge the effective Stokes' shift and provides a range of excitation wavelengths that can be utilized for sensor technology.

Coordination of protons to the pyridine N atom switches on an intramolecular charge-transfer reaction and thereby decreases the amount of fluorescence from the BODIPY unit. Complexation can also be followed by absorption spectroscopy as the bands associated with the BODIPY unit undergo a modest red shift. Because absorption transitions localized on the perylene units are insensitive to cation coordination, the spectral shift decreases the rate of through-space electronic energy transfer and restores some fluorescence from the perylene residues. Pyridine is a relatively weak and indiscriminate coordinative group and will bind to most cations. This situation cannot be exploited to design sensitive and/or selective fluorescent sensors but is ideal for a remote probe intended to provide a termination signal if cations leak from a reactor due to a ruptured membrane or seal. As a further safeguard, we note that the decreased fluorescence from BODIPY is accompanied by increased emission from the perylene units. This type of orthogonal sensing has many attractions.

Experimental Section

General Methods: 200.1 (^1H), 300.1 (^1H), 400 (^1H), 50.3 (^{13}C), 75.46 (^{13}C) and 100.3 (^{13}C) MHz NMR spectra were recorded at room temperature using the residual proton resonances in deuterated solvents as internal references. The 128.4 MHz ^{11}B NMR spectra were recorded at room temperature with B in borosilicate glass as reference ($\text{BF}_3 \cdot \text{Et}_2\text{O}$ value 3.18 ppm). Fast-atom bombardment mass spectra were obtained using a ZAB-HF-VB-analytical apparatus in positive mode with *m*-nitrobenzyl alcohol (*m*NBA) as matrix. Chromatographic purification was conducted using standardized silica gel or aluminium oxide. Thin-layer chromatography (TLC) was performed on silica gel or aluminium oxide plates coated with fluorescent indicator. All mixtures of solvents are given in v/v ratio.

Materials: Samples of CH_2Cl_2 were distilled from P_4O_{10} and tetrahydrofuran (THF) from Na/benzophenone. Kryptopyrrole, EtMgBr, tolylacetylene, Et_3N and $\text{BF}_3 \cdot \text{Et}_2\text{O}$ were used as purchased. 1-Ethynylperylene was obtained by a literature procedure.^[29]

2,6-Diethyl-4,4-difluoro-1,3,5,7-tetramethyl-8-(4-pyridinyl)-4-bora-3a,4a-diaza-s-indacene (1): Kryptopyrrole (330 μL , 2.4 mmol) was stirred with 4-(chlorocarbonyl)pyridine (0.216 g, 1.2 mmol) in CH_2Cl_2 , at room temperature during 4 d. The solution turned deep red. The resultant dipyrromethene solution was deprotonated with triethylamine (1.0 mL), boron trifluoride-diethyl ether (1.2 mL) was added, and the solution stirred for 3 h. The resulting organic mixture was washed with a saturated NaHCO_3 aqueous solution, dried with MgSO_4 , and the solvent removed. Column chromatography on alumina (Act IV, hexane/dichloromethane, with a gradient from 8:2 to 5:5) afforded the desired compound as a red powder (0.184 g, 40%). M.p. 168–169 $^\circ\text{C}$. ^1H NMR (400 MHz, CDCl_3): δ = 0.99 (t, 3J = 7.6 Hz, 6 H), 1.32 (s, 6 H), 2.31 (q, 3J = 7.6 Hz, 4 H), 2.55 (s, 6 H), 7.31 (dd, 3J = 4.3, 4J = 1.5 Hz, 2 H), 8.78 (dd, 3J = 4.5, 4J = 1.7 Hz, 2 H) ppm. $^{13}\text{C}\{^1\text{H}\}$ NMR (100.6 MHz, CDCl_3): δ = 12.3 (CH_3), 13.0 (CH_3), 15.0 (CH_3), 17.5 (CH_2), 124.1 (CH), 130.1 (Cq), 133.8 (Cq), 136.6 (Cq), 138.2 (Cq), 144.8 (Cq), 151.0 (CH), 155.2 (Cq) ppm. ^{11}B NMR (128.4 MHz, CDCl_3): δ = 3.79 (t, $^1J_{\text{B-F}}$ = 32.8 Hz) ppm. UV/Vis (CH_2Cl_2 , 23 $^\circ\text{C}$): λ_{max} (ϵ , $\text{M}^{-1}\text{cm}^{-1}$) = 235 (14800), 382 (6300), 501 (sh, 21000), 528 (59000). IR (KBr): $\tilde{\nu}$ = 1638 (s, $\nu_{\text{C=N}}$), 1414, 1118 cm^{-1} . MS (FAB $^+$, *m*NBA):

m/z (%) = 382.2 (30) [$\text{M} + \text{H}^+$], 381.2 (100) [M], 362.3 (20) [$\text{M} - \text{F}$] $^+$. $\text{C}_{22}\text{H}_{26}\text{BF}_2\text{N}_3$ (381.27): calcd. C 69.30, H 6.87, N 11.02; found C 69.10, H 6.61, N 10.82.

General Procedure for Substitution of Fluoride by Acetylide: In a Schlenk flask, ethylmagnesium bromide (2.2 equiv.) was added to a stirred, degassed solution of the acetylenic compound (2.5 equiv.) in anhydrous THF held at room temp. The mixture was heated at 60 $^\circ\text{C}$ for 2 h. The resulting anion was then transferred via cannula to a degassed solution of the precursor difluoroboradiaindacene (1 equiv.) in anhydrous THF. The solution was stirred at 60 $^\circ\text{C}$ for 18 h. Water was added, and the solution was extracted with CH_2Cl_2 . After evaporation, the organic layer was purified by column chromatography and recrystallized from CH_2Cl_2 /hexane.

2,6-Diethyl-1,3,5,7-tetramethyl-8-(pyridin-4-yl)-4,4-bis(*p*-tolylethynyl)-4-bora-3a,4a-diaza-s-indacene (2): Prepared according to the general procedure with 4-ethynyltoluene (0.046 mL, 0.36 mmol) in 2 mL of THF, 0.30 mL of EtMgBr (1 M in THF), and **1** (0.046 g, 0.12 mmol) in 2 mL of THF. Chromatography was carried out on silica (CH_2Cl_2 /petroleum ether, 20:80), and followed by a recrystallization (CH_2Cl_2 /cyclohexane) to afford 18 mg of **2** (26% yield). ^1H NMR (CDCl_3 , 300 MHz): δ = 8.74 (br. s, 2 H), 7.41 (br. s, 2 H), 7.17 (AB system, 8 H, J_{AB} = 8.0 Hz, δ = 75.2), 2.86 (s, 6 H), 2.35 (t, 3J = 7.5 Hz, 4 H), 2.31 (s, 6 H), 1.32 (s, 6 H), 1.02 (t, 3J = 7.5 Hz, 6 H) ppm. $^{13}\text{C}\{^1\text{H}\}$ NMR (CDCl_3 , 75 MHz): δ = 154.7, 136.9, 136.1, 135.5, 133.4, 131.4, 128.7, 128.0, 122.3, 30.9, 29.6, 21.4, 17.4, 14.7, 14.1, 12.1 ppm. EI-MS: m/z (nature of peak, relative intensity): 574.2 (100) [$\text{M} + \text{H}^+$], 458.2 (20) [$\text{M} - \text{tol} \equiv$]. $\text{C}_{40}\text{H}_{40}\text{BN}_3$ (573.59): calcd. C 83.76, H 7.03, N 7.33; found C 83.45, H 6.89, N 7.09.

2,6-Diethyl-1,3,5,7-tetramethyl-4,4-bis(1-perylenylethynyl)-8-(pyridin-4-yl)-4-bora-3a,4a-diaza-s-indacene (3): Prepared according to the general procedure with 1-ethynylperylene (0.103 g, 0.37 mmol) in 2 mL of THF, 0.35 mL of EtMgBr (1 M in THF), and **1** (0.062 g, 0.16 mmol) in 2 mL of THF. Chromatography was performed on silica (CH_2Cl_2 /petroleum ether, 20:80), and recrystallization (CH_2Cl_2 /cyclohexane) gave 0.04 g of **3** (27% yield). ^1H NMR (CDCl_3 , 300 MHz): δ = 8.81 (br. s, 2 H), 8.42 (d, 3J = 8.3 Hz, 2 H), 8.22–8.08 (m, 8 H), 7.69–7.64 (m, 6 H), 7.53–7.44 (m, 8 H), 3.07 (s, 6 H), 2.44 (q, 3J = 7.5 Hz, 4 H), 1.41 (s, 6 H), 1.10 (t, 3J = 7.5 Hz, 6 H) ppm. $^{13}\text{C}\{^1\text{H}\}$ NMR (CDCl_3 , 75 MHz): δ = 154.7, 150.4, 145.0, 136.4, 135.9, 135.2, 134.7, 133.7, 131.4, 131.2, 131.0, 130.6, 130.5, 128.6, 128.5, 128.3, 127.9, 127.8, 126.9, 126.7, 126.6, 126.5, 124.1, 122.6, 120.5, 120.3, 119.7, 94.3, 17.4, 14.8, 14.6, 12.2 ppm. ^{11}B $\{^1\text{H}\}$ NMR (CDCl_3 , 128 MHz): δ = –8.97 (s) ppm. EI-MS: m/z (nature of peak, relative intensity): 893.2 (100) [M^+], 618.2 (35) [$\text{M} - \text{peryl} \equiv$]. $\text{C}_{66}\text{H}_{48}\text{BN}_3$ (893.94): calcd. C 88.68, H 5.41, N 4.70; found C 88.39, H 5.17, N 4.35.

Spectroscopic Studies: All solvents were purchased at spectroscopic grade from Aldrich Chemicals Co., used as received, and were found to be free of fluorescent impurities. Absorption spectra were measured with a Hitachi U3310 spectrophotometer, corrected with baseline changes and converted to molar absorption coefficient using the Beer–Lambert law, averaging over a series of dilute measurements of known concentration recorded at room temperature. Fluorescence spectra were measured with a fully-corrected Jobin–Yvon Fluorolog tau-3 spectrometer for quantitative measurements and a Hitachi F-4500 fluorescence spectrometer for routine spectra. Fluorescent measurements were obtained using optically dilute solutions with an absorbance less than or equal to 0.1 at the excitation wavelength. Fluorescence quantum yields were measured at room temperature in CH_2Cl_2 solution relative to perylene (Φ_{F} = 0.79),^[11] excited at 408 nm, or **1** (Φ_{F} = 0.88), excited at 500 nm.^[9]

Lifetime measurements were made using a PTI EasyLife spectrometer using Ludox in distilled water to measure the instrumental response function. Analysis of the experimental data consists of deconvolution against the instrumental response function and fitting to sums of exponentials. A combination of iterative re-convolution and nonlinear least-squares fits was used. Synthetic data by which to test the reliability of the analysis were generated by numerical convolution. Excitation wavelengths of 440 nm (perylene and BODIPY) and 525 nm (BODIPY) were used and any fluorescence was resolved with a high radiance monochromator after passing through suitable non-emissive filters. The temporal resolution of the instrument is ca. 50 ps after signal averaging.

Fast transient spectroscopy was carried out by pump-probe techniques using fs pulses delivered from a Ti:sapphire generator amplified with a multi-pass amplifier pumped via the second harmonic of a Q-switched Nd:YAG laser. The amplified pulse energies varied from 0.3 to 0.5 mJ and the repetition rate was kept at 10 Hz. Part of the beam (ca. 20%) was focused onto a second harmonic generator in order to produce the excitation pulse. The residual output was directed onto a 4-mm sapphire plate so as to create a white light continuum for detection purposes. The continuum was collimated and split into two equal beams. The first beam was used as reference whilst the second beam was combined with the excitation pulse and used as the diagnostic beam. The two beams were directed to different parts of the entrance slit of a cooled CCD detector and used to calculate differential absorbance values. The CCD shutter was kept open for 1 s and the accumulated spectra were averaged. This procedure was repeated until about 100 individual spectra had been averaged. Time-resolved spectra were recorded with a delay line stepped in increments of 100 fs. The sample, possessing an absorbance of ca. 1 at 420 nm, was flowed through a quartz cuvette (optical pathlength: 2 mm) and maintained under N₂.

High-pressure studies were conducted with a special rig constructed by Stansted Fluid Power Ltd. The sample, housed in a glass capillary tube, was subjected to increasing pressure applied via hydraulic means. The sample was excited with a high power 408 nm laser diode and isolated from scattered light using glass filters. The signal was transferred to the Hitachi spectrophotometer for averaging and data storage.

Acknowledgments

This work received financial support from the Engineering and Physical Sciences Research Council (EPSRC) (EP/D053080/1), Centre National de la Recherche Scientifique (CNRS), Université Louis Pasteur de Strasbourg, and Newcastle University. G. U. thanks the Agence Nationale de la Recherche (ANR) "Borsup-stokes", project JC05-4228, for further financial support.

- [1] *Fluorescence Sensors and Biosensors* (Ed.: R. B. Thompson) Taylor & Francis CRC Press, London, **2005**.
- [2] a) B. R. Eggins, *Chemical Sensors and Biosensors*, Wiley, Chichester, **2002**; b) *Chemosensors of Ion and Molecule Recognition* (Eds.: J. P. Desvergne, A. W. Czarnik), NATO Science Series C, **1997**.
- [3] a) J.-P. Malval, I. Leray, B. Valeur, *New J. Chem.* **2005**, 29, 1089–1094; b) L. Zeng, E. W. Miller, C. J. Chang, A. Pralle, E. Y. Isacoff, *J. Am. Chem. Soc.* **2006**, 128, 10–11; c) M. Baruah, W. Qin, R. A. L. Vallée, D. Beljonne, T. Rohand, W. Dehaen, N. Boens, *Org. Lett.* **2005**, 7, 4377–4380; d) N. Basarić, M. Baruah, W. Qin, B. Metten, M. Smet, W. Dehaen, N. Boens, *Org. Biomol. Chem.* **2005**, 3, 2755–2761; e) X. Peng, Y. Xu, S. Sun, Y. Wu, J. Fan, *Org. Biomol. Chem.* **2007**, 5, 226–228; f) N. Malatesti, R. Hudson, K. Smith, H. Savoie, K. Rix, K. Welham, R. W. Boyle, *Photochem. Photobiol.* **2006**, 86, 746–749.
- [4] R. A. Bissell, A. P. Da Silva, H. Q. N. Gunaratne, P. L. M. Lynch, G. E. M. Maguire, C. P. McCoy, K. R. A. S. Sandanayake, *Top. Curr. Chem.* **1993**, 168, 223–264.
- [5] a) W. Wang, G. Springsteen, S. Gao, B. Wang, *Chem. Commun.* **2000**, 1283–1284; b) I. Grabchev, X. Qian, Y. Xiao, R. Zhang, *New J. Chem.* **2002**, 26, 920–925; c) J. Wang, X. Qian, *Org. Lett.* **2006**, 8, 3721–3724.
- [6] a) R. Ziessel, G. Ulrich, A. Harriman, *New J. Chem.* **2007**, 31, 496–501; b) A. Loudet, K. Burgess, *Chem. Rev.* **2007**, 107, 4891–4932; c) G. Ulrich, R. Ziessel, A. Harriman, *Angew. Chem. Int. Ed.* **2008**, 47, 1184–1201.
- [7] R. Ziessel, C. Goze, G. Ulrich, M. Cesario, P. Retailleau, A. Harriman, J. P. Rostron, *Chem. Eur. J.* **2005**, 11, 7366–7378.
- [8] C. Goze, G. Ulrich, L. J. Mallon, B. D. Allen, A. Harriman, R. Ziessel, *J. Am. Chem. Soc.* **2006**, 128, 10231–10239.
- [9] A. Harriman, L. J. Mallon, G. Ulrich, R. Ziessel, *ChemPhysChem* **2007**, 8, 1207–1214.
- [10] G. Ulrich, R. Ziessel, *J. Org. Chem.* **2004**, 69, 2070–2083.
- [11] J. H. Malkin, *Photophysical and Photochemical Properties of Aromatic Compounds*, Taylor & Francis CRC Press, London, **1992**.
- [12] a) W. Qin, T. Rohand, M. Baruah, A. Stefan, M. Van der Auweraer, W. Dehaen, N. Boens, *Chem. Phys. Lett.* **2006**, 420, 562–568; b) T. Rohand, J. Lycoops, S. Smout, E. Braeken, M. Sliwa, M. Van der Auweraer, W. Dehaen, W. M. De Borggraeve, N. Boens, *Photochem. Photobiol. Sci.* **2007**, 6, 1061–1066.
- [13] K. Rurack, M. Kollmannsberger, J. Daub, *New J. Chem.* **2001**, 25, 289–294.
- [14] S. J. Strickler, R. A. Berg, *J. Chem. Phys.* **1962**, 37, 814–820.
- [15] a) S. Zrig, P. Rémy, B. Andrioletti, E. Rose, I. Asselberghs, K. Clays, *J. Org. Chem.* **2008**, 73, 1563–1566; b) M. D. Yilmaz, O. A. Bozdemir, E. U. Akkaya, *Org. Lett.* **2006**, 8, 2871–2873; c) A. Burghart, L. H. Thoresen, J. Chen, K. Burgess, F. Bergström, L. B.-A. Johansson, *Chem. Commun.* **2000**, 2203–2204; d) S. C. Hung, R. A. Mathies, A. N. Glazer, *Anal. Biochem.* **1998**, 255, 32–38.
- [16] a) G. S. Jiao, L. H. Thoresen, T. G. Kim, W. C. Haaland, F. Gao, M. R. Topp, R. M. Hochstrasser, M. L. Metzker, K. Burgess, *Chem. Eur. J.* **2006**, 12, 7816–7826; b) R. Bandichhor, A. D. Petrescu, A. Vespa, A. B. Kier, F. Schroeder, K. Burgess, *J. Am. Chem. Soc.* **2006**, 128, 10688–10689; c) T. G. Kim, J. C. Castro, A. Loudet, G. S. Jiao, R. M. Hochstrasser, M. R. Topp, K. Burgess, *J. Phys. Chem. A* **2006**, 110, 20–27.
- [17] A. Harriman, G. Izzet, R. Ziessel, *J. Am. Chem. Soc.* **2006**, 128, 10868–10875.
- [18] F. Li, S. I. Yang, Y. Ciringh, J. Seth, C. H. Martin III, D. L. Singh, D. Kim, R. R. Birge, D. F. Bocian, D. Holten, J. S. Lindsey, *J. Am. Chem. Soc.* **1998**, 120, 10001–10009.
- [19] B. Y. Okamoto, H. G. Drickamer, *Proc. Natl. Acad. Sci. USA* **1974**, 71, 4757–4759.
- [20] a) J. H. Eggert, L.-W. Xu, R.-Z. Che, L.-C. Chen, J.-F. Wang, *J. Appl. Phys.* **1992**, 72, 2453–2459; b) T. Takagi, H. Teranishi, *J. Chem. Eng. Data* **1982**, 27, 16–18.
- [21] H. L. Kee, C. Kirmaier, L. Yu, P. Thamyongkit, W. J. Youngblood, M. E. Calder, L. Ramos, B. C. Noll, D. F. Bocian, W. R. Scheidt, R. R. Birge, J. S. Lindsey, D. Holten, *J. Phys. Chem. B* **2005**, 109, 20433–20443.
- [22] a) J. S. McCaskill, R. G. Gilbert, *Chem. Phys.* **1979**, 44, 389–402; b) A. D. Osborne, *J. Chem. Soc. Faraday Trans. 2* **1980**, 76, 1638–1645; c) D. Ben-Amotz, C. B. Harris, *J. Chem. Phys.* **1987**, 86, 4856–4870.
- [23] R. Englman, J. Jortner, *Mol. Phys.* **1970**, 18, 145–164.
- [24] a) N. Saki, T. Dinc, E. U. Akkaya, *Tetrahedron* **2006**, 62, 2721–2725; b) W. Qin, M. Baruah, M. Van der Auweraer, F. C. De Schryver, N. Boens, *J. Phys. Chem. A* **2005**, 109, 7371–7384; c) M. Baruah, W. Qin, C. Flors, J. Hofkens, R. A. L. Vallée,

- D. Beljonne, M. Van der Auweraer, W. M. De Borggraeve, N. Boens, *J. Phys. Chem. A* **2006**, *110*, 5998–6009; d) W. Qin, M. Baruah, A. Stefan, M. Van der Auweraer, N. Boens, *ChemPhysChem* **2005**, *7*, 2343–2351; e) M. Baruah, W. Qin, N. Basarić, W. M. De Borggraeve, N. Boens, *J. Org. Chem.* **2005**, *70*, 4152–4157.
- [25] A. Harriman, J. P. Rostron, M. Cesario, G. Ulrich, R. Ziessel, *J. Phys. Chem. A* **2006**, *110*, 7994–8002.
- [26] X. Zhang, Y. Xiao, X. Qian, *Org. Lett.* **2008**, *10*, 29–32.
- [27] a) B. Turfan, E. U. Akkaya, *Org. Lett.* **2002**, *4*, 2857–2859; b) Y. Gabe, Y. Urano, K. Kikuchi, H. Kojima, T. Nagano, *J. Am. Chem. Soc.* **2004**, *126*, 3357–3367; c) K. Rurack, M. Kollmannsberger, U. Resch-Genger, J. Daub, *J. Am. Chem. Soc.* **2000**, *122*, 968–969; d) A. Coskun, B. T. Baytekin, E. U. Akkaya, *Tetrahedron Lett.* **2003**, *44*, 5649–5651; e) A. Coskun, E. U. Akkaya, *J. Am. Chem. Soc.* **2005**, *127*, 10464–10465; f) K. Rurack, M. Kollmannsberger, J. Daub, *Angew. Chem. Int. Ed.* **2001**, *40*, 385–387.
- [28] A. Harriman, L. J. Mallon, S. Goeb, R. Ziessel, *Phys. Chem. Chem. Phys.* **2007**, *9*, 5199–5201.
- [29] M. Inouye, Y. Hyodo, H. Nakazumi, *J. Org. Chem.* **1999**, *64*, 2704–2710.

Received: February 9, 2008
Published Online: April 15, 2008